HHS Public Access

Author manuscript

Mol Cell. Author manuscript; available in PMC 2018 January 05.

Published in final edited form as:

Mol Cell. 2017 January 05; 65(1): 154–167. doi:10.1016/j.molcel.2016.11.034.

A constitutive intrinsic inflammatory signaling circuit composed of miR-196b, Meis2, PPP3CC, and p65, drives prostate cancer castration-resistance

Ji-Hak Jeong[1], **Sun-Jin Park**[1], **Shohreh Iravani Dickinson**[2], and **Jun-Li Luo**[1,*]

[1]Department of Cancer Biology, The Scripps Research Institute, Jupiter, FL 33458, USA

[2]Department of Pathology, Moffitt Cancer Center, 2902 Magnolia Drive, Tampa, FL 33612, USA

SUMMARY

Androgen deprivation therapy is the most effective treatment for advanced prostate cancer, however, almost all cancer eventually become castration-resistant, and the underlying mechanisms are largely unknown. Here, we show that an intrinsic constitutively activated feed-forward signaling circuit composed of IκBα/NF-κB(p65), miR-196b-3p, Meis2, PPP3CC is formed during the emergence of castration-resistant prostate cancer (CRPC). This circuit controls the expression of stem cell transcription factors that drives the high tumorigenicity of CRPC cells. Interrupting the circuit by targeting its individual components significantly impairs the tumorigenicity and CRPC development. Notably, constitutive activation of IκBα/NF-κB(p65) in this circuit is not dependent on the activation of traditional IKKβ/NF-κB pathways that are important in normal immune responses. Therefore, our studies present deep insight into the bona fide mechanisms underlying castration-resistance and provide the foundation for the development of CRPC therapeutic strategies that would be highly efficient while avoiding indiscriminate IKK/NF-κB inhibition in normal cells.

Graphical Abstract

*Corresponding Author and Lead Contact: jlluo@scripps.edu.

AUTHOR CONTRIBUTIONS

S.I.D. and J.L.L. conceived the project. J.H.J. performed most experiments and analyzed results. S.J.P. helped with kinase assay and immunohistochemistry studies. S.I.D. helped with human samples and pathology studies. J.H.J. and J.L.L. wrote the manuscript with input from all authors.

COMPETING FINANCIAL INTERESTS

The authors declare no competing financial interests.

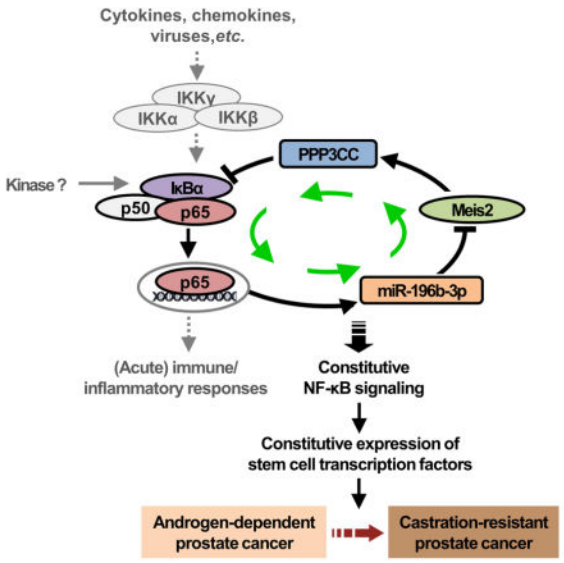

INTRODUCTION

Prostate cancer (PCa) is the most common malignancy, and the second-leading cause of cancer-related mortality in men in Western countries (Amaral et al., 2012; Karantanos et al., 2013). In tumors confined to the prostate, radical prostatectomy and radiotherapy are effective, however, for late stage disseminated disease, current therapies are merely palliative (Amaral et al., 2012). Androgen receptor (AR) signaling is a critical survival pathway for prostate cancer cells, and androgen deprivation therapy (ADT) is an initial systemic therapy for advanced PCa and is also used as an adjuvant to local therapy for high-risk diseases. Although a majority of patients initially respond to ADT, the responses in advanced disease are transient and almost all eventually develop castration resistance (Alibhai et al., 2006; Amaral et al., 2012; Karantanos et al., 2013). Castration-resistant prostate cancer (CRPC) is associated with a very poor prognosis, and the treatment of which remains a serious clinical challenge (Alibhai et al., 2006; Amaral et al., 2012; Karantanos et al., 2013). Understanding the mechanisms that underlie the pathogenesis of castrate resistance is therefore needed to develop novel therapeutic approaches for this disease.

Inflammatory signaling has been linked to various cancers. However, how it is constitutively activated and maintained in cancer cells and its difference from normal immune responses are largely unknown (Coussens and Werb, 2002; Grivennikov et al., 2010; Iliopoulos et al., 2009; Rokavec and Luo, 2012; Rokavec et al., 2012). NF-κB transcription factors play essential roles in the regulation of innate and adaptive immune responses, inflammation, and cell survival (Delhase and Karin, 1999). A number of stimuli activate NF-κB, mostly through IκB kinase (IKK)-dependent phosphorylation and subsequent degradation of the IκB inhibitory proteins. The IKK complex consists of two highly homologous kinase subunits (IKKα and IKKβ) and a nonenzymatic regulatory component, IKKγ/NEMO (Ghosh and Karin, 2002). There are two NF-κB activation pathways. The classical NF-κB activation pathway is triggered in response to microbial and viral infections and exposure to

proinflammatory cytokines that activate the tripartite IKK complex leading to phosphorylation-induced degradation of IκBs. This pathway depends mainly on the IKKβ catalytic subunit (Ghosh and Karin, 2002; Luo et al., 2005). The alternative pathway leads to selective activation of p52:RelB NF-κB dimers by inducing processing of the NF-κB2/p100 precursor that binds to the RelB NF-κB subunit in the cytoplasm (Ghosh and Karin, 2002; Luo et al., 2005). As NF-κB plays important roles in tumorigenesis, progression, and metastasis, it has been regarded as one of the most important targets for cancer therapy (Karin, 2006; Luo et al., 2005; Perkins, 2012). However, the application of IKK/NF-κB inhibitors for the treatment of human cancer is impeded by severe side effects related to immunosuppression, due to the indiscriminate inhibition of IKK/NF-κB in normal immune cells. Therefore, the strategies that specifically targeting NF-κB activity only in tumor cells while sparing NF-κB immune response in normal cells would be highly desirable.

Here, by investigating the primary cells directly isolated from mouse primary or castration-resistant allograft/xenograft prostate tumors and analyzing human prostate tumors, we report that a constitutively activated signaling circuit composed of IκBα/NF-κB(p65), miR-196b-3p, Meis2, PPP3CC is formed intrinsically in prostate cancer cells during the emergence of CRPC. This constitutive signaling circuit drives the high tumorigenicity and aggressiveness of CRPC. Importantly, although IκBα/NF-κB(p65) are included in this signaling circuit, the constitutive activation of NF-κB in the circuit is not dependent on traditional IKKβ/NF-κB activation pathways. Thus, our studies provide the foundation for the development of therapeutic strategies that target constitutive NF-κB specifically in tumor cells while avoid NF-κB inhibition in normal immune cells.

RESULTS

Castration-resistant prostate cancer (CRPC) cells are much more tumorigenic than primary prostate cancer (PPC) cells

To investigate the mechanisms underlying castration-resistant prostate cancer (CRPC) development, we employed a prostate cancer (PCa) allograft mouse model that mimics human CRPC development (Ammirante et al., 2010; Watson et al., 2005). In this model, an androgen-dependent (AD) mouse prostate cancer cell line, Myc-CaP, which was isolated from a *c-Myc* transgenic prostate cancer mouse with PCa (Watson et al., 2005), was employed. Myc-CaP cells can grow as tumors in immune competent FVB mice in an AD manner, when host mice are castrated, Myc-CaP allografts shrink, and later re-grow and become AR-positive CRPC (Figure S1A). To compare the tumorigenicity of CRPC cells and primary prostate cancer (PPC) cells, primary cells from PPC and CRPC tumors were isolated. Cells with different dilutions were then inoculated into FVB male mice for tumor development (Figure 1A). We found that five CRPC cells were enough to initiate a tumor at about 30 days after inoculation, while mice inoculated with five cells of cultured Myc-CaP or PPC cells did not develop tumor during 2-years of observation time. Although all mice inoculated with 10 cells of CRPC, PPC, or cultured Myc-CaP cells developed tumor, the tumor onsets for each cell type were very different, with CRPC cells developing tumors at about 30 days, PPC cells at about 60 days, and cultured Myc-CaP cells at about 100 days after inoculation (Figures 1A, S1B, and S1C). These results suggest that primary cells

isolated from CRPC are much more tumorigenic than the primary cells from PPC. Consistently, CRPC cells proliferated and migrated much more rapidly (Figure 1B and 1C), and formed much more colonies in soft agar (Figure 1D) and tumor spheres in suspension culture (Figure 1E) than PPC cells.

It should be emphasized that the primary cells from PPC had much stronger tumorigenicity than the cultured Myc-CaP cells, suggesting cultured tumor cell lines have lost some properties of original tumor cells in the tumor mass. Therefore, Cancer cells directly purified from PPC or CRPC tumors (thereafter called PPC cells or CRPC cells) are much more representative than cultured Myc-CaP cell line. All our experiments were carried out in PPC and CRPC cells, and cultured Myc-CaP cell line was used for control purpose.

CRPC cells express much higher levels of stem cell markers than PPC cells

As tumorigenicity is related to stemness of cancer cells, we analyzed the expression of the prostate cancer stem cell markers, CD49f and Sca-1 (Mulholland et al., 2009; Xin et al., 2005), in PPC and CRPC cells by qRT-PCR, and found that the expression of *CD49f* and *Sca-1* mRNA in CRPC cells were significantly higher than PPC cells (Figure 1F). We also measured the percentage of positive CD49f and Sca-1 cells in PPC and CRPC cells by FACS analysis, and found that about 99% CRPC cells while only about 5% PPC cells were both CD49f and Sca-1 positive (Figure 1G and S1D). These results indicate CRPC cells have much more cancer stem-like cell populations than PPC cells.

IKKβ-independent NF-κB (p65) constitutive activation drives the tumorigenicity of CRPC cells

To understand the underlying mechanisms by which CRPC cells are more tumorigenic than PPC cells, we employed a kinase inhibitor library to identify kinase(s) that promotes the tumorigenicity in CRPC cells. We found that CRPC cells were much more sensitive than PPC cell to the treatment of inhibitors, BAY11-7082 or Celastrol, which can inhibit IκBα or NF-κB (Figure 2A and S2A). However, PPC, CRPC, and cultured Myc-CaP cells had similar sensitivities to other kinase inhibitors, including SC 514 that can inhibit IKKβ (Figure 2A and S2A). We found that the phosphorylation of IκBα and the activity of NF-κB (p65) were increased in CRPC cells as compared with PPC cells (Figure 2B, 2C, and S2B–D). Although both SC 514 and BAY 11-7082 blocked LPS-induced expression of p-IκBα in both PPC and CRPC cells (Figure S2E), BAY 11-7082 decreased the basal levels of p-IκBα expression and NF-κB DNA binding activity while SC 514 had no such effect in CRPC cells (Figure S2E and S2F). Furthermore, IKKβ and IKK complex immunoprecipitated from PPC and CRPC cells had similar activity in the phosphorylation of GST-IκBα (1–54) *in vitro* (Figure S2G).

Consistently, inhibition of IκBα and NF-κB by inhibitors or p65 knockdown by p65 siRNA significantly decreased CRPC cells' viability (Figure 2A, S2H, and S2I), colony formation in soft agar (Figure 2D, S2H, and S2J), and tumor sphere formation in suspension culture (Figure 2E, S2H, and S2K) while inhibition of IKKβ by inhibitor or IKKβ knockdown by IKKβ siRNA had no such effects on CRPC cells (Figure 2A, S2H–K). We also found that NF-κB/p65 stable knockdown did not affect the initiation and development of primary

tumors (PPC) (Figure 2F, and S2L), whereas p65 knockdown significantly suppressed CRPC development (Figure 2F, and S2O–Q). In contrast, IKKβ knockdown neither affected the initiation and development of PPC nor the development of CRPC (Figure 2G, S2M–N, S2R, and S2S). These results indicate that constitutive activated NF-κB (p65) drives CRPC development, which is not dependent on IKKβ.

Previous reports suggest that nuclear IKKα plays a crucial role in prostate cancer progression and metastasis (Ammirante et al., 2013; Ammirante et al., 2010; Luo et al., 2007). A recent report suggests that a fraction of phosphorylated and sumoylated IκBα binds to the chromatin and regulates a subset of polycomb target genes in keratinocytes (Mulero et al., 2013). We found that although the expression of nuclear IKKα and nuclear p-IKKα/β was increased in CRPC cells, IκBα did not translocate to nuclei of both CRPC and PPC cells (Figure S2T and S2U), suggesting that nuclear IKKα is not related to the increased p-IκBα in CRPC cells.

Constitutive NF-κB (p65) activation in CRPC is controlled by PPP3CC-mediated down-regulation of p-IκBα

The NF-κB (p65) activation is usually regulated by IKKβ-mediated phosphorylation of IκBs (Luo et al., 2005). However, our results suggest that the constitutive IκBα phosphorylation and NF-κB (p65) activation in CRPC cells are not dependent on IKKβ (Figure 2A, 2D, 2E, S2E–K, and S2U). To investigate how IκBα/NF-κB(p65) is constitutively activated in CRPC cells, a phosphatase inhibitor library was employed to screen the phosphatase(s) that contribute to the constitutive IκBα phosphorylation in CRPC cells. We found that treatment with the phosphatase inhibitors, Cypermethrin and Deltamethrin, which inhibit serine/threonine-protein phosphatase 2b (PP2B), increased p-IκBα expression and p65 activity in PPC cells (Figure 3A, 3B, and S3A). However, the increased phosphorylation of IκBα after PP2B inhibition is not dependent on IKKβ (Figure S3B).

PP2B, also called Calcineurin (CN), consists of a catalytic subunit (CNA) and a regulatory subunit (CNB) (Shi, 2009). CNA has three isoforms: CNAα (PPP3CA), CNAβ (PPP3CB), and CNAγ (PPP3CC), while CNB has two isoforms: CNBα (PPP3R1) and CNBβ (PPP3R2). We found that the expression of PPP3CC mRNA (Figure S3C) and protein (Figure 3C) was down regulated in CRPC cells as compared with PPC cells, whereas there were no differences in the expression of other PP2B catalytic isoforms between PPC and CRPC cells (Figure S3C). Furthermore, we found that PPP3CC knockdown significantly increased the expression of p-IκBα (Figure 3D) and enhanced the activity of p65 in PPC cells (Figure 3E), while overexpression of PPP3CC resulted in decreased p-IκBα expression (Figure 3F) and reduced p65 activity in CRPC cells (Figure 3G). In addition, PPP3CC can directly dephosphorylate p-IκBα *in vitro* (Figure 3H). These results suggest that PPP3CC down-regulation contributes to the constitutive IκBα phosphorylation and p65 activation in CRPC cells (Figure S3D).

Importantly, we found that overexpression of PPP3CC in CRPC cells decreased while knockdown of PPP3CC in PPC cells increased colony formation in soft agar (Figure 3I, 3K, and S3E–J) and tumor sphere formation in suspension culture (Figure 3J, 3L, and S3K). Overexpression of p65 restored the colony and tumor sphere formation capability of

PPP3CC-overexpression CRPC cells in soft agar (Figure S3L and S3M) and in suspension culture (Figure S3N). We also found that stable overexpression of PPP3CC significantly suppressed CRPC development in FVB allograft mouse models (Figure 3M and S3O–P). These results suggest that PPP3CC functions as a tumor suppressor in CRPC development.

Constitutive NF-κB (p65) induces the expression of miR-196b-3p in CRPC

We screened miRNA expression in Myc-CaP, PPC, and CRPC cells by miRNA array analysis, and found that the expression of a group of miRNAs had more than two times difference between CRPC and PPC cells (Figure 4A, S4A, and S4B). To examine whether the differential expression of these miRNAs is related to constitutive NF-κB (p65) activation in CRPC cells, p65 was knocked down in CRPC cells by p65 siRNA and the expression of these miRNAs were examined. We found that knockdown of p65 significantly decreased the expression of both primary and mature miR-196b-3p while the expression levels of other miRNAs were not significantly changed (Figure 4B and S4C). Consistently, overexpression of p65 in PPC cells increased the expression of primary and mature miR-196b-3p (Figure 4C and S4D). Furthermore, we found that the expression of primary and mature miR-196b-3p was significantly decreased in castration-resistant allograft tumors derived from p65 stable knockdown Myc-CaP cells (Figure 4D and S4E). These results indicate that constitutively activated p65 controls the expression of miR-196b-3p in CRPC cells.

To examine whether p65 binds to the promoter of miR-196b, chromatin immunoprecipitation (ChIP) assays were performed in PPC and CRPC cells (Table S1). We found that the binding of p65 to miR-196b promoter at −592 ~ −422 region was significantly increased in CRPC cells as compared with PPC cells (Figure 4E and S4F), suggesting that p65 binds to miR-196b-3p promoter and regulates its expression in CRPC cells.

Since our findings showed that PPP3CC suppressed IκBα phosphorylation and NF-κB (p65) activation (Figure 3D–G), we asked whether PPP3CC also regulates the expression of miR-196b-3p in CRPC. As expected, knockdown of PPP3CC in PPC cells increased miR-196b-3p expression (Figure S4G), while overexpression of PPP3CC in CRPC cells decreased miR-196b-3p expression (Figure S4H). We then asked whether the regulation of PPP3CC on miR-196b-3p is mediated by p65. PPC cells were transfected with PPP3CC siRNA to knock down PPP3CC, followed by transfection with p65 siRNA, 48 hr later the expression of miR-196b-3p were examined. We found knockdown of PPP3CC in PPC cells increased the activity of p65 and the expression of miR-196b-3p, knockdown of p65 blocked the induction of miR-196b-3p (Figure 4F). Similarly, we found that overexpression of PPP3CC in CRPC cells decreased the activity of p65 and the expression of miR-196b-3p, restoring the p65 activity by overexpression of p65 blocked the reduction of miR-196b-3p expression (Figure 4G). These results suggest that PPP3CC controls p65-directed induction of miR-196b-3p (Figure S4I).

Furthermore, we found that miR-196b overexpression cells formed more colonies in soft agar (Figure 4H, S4J, and S4K) and had more tumor sphere formation than control cells (Figure 4I). MiR-196b overexpression cells developed CRPC much more rapidly than control cells in castrated FVB mice (Figure 4J, S4L, and S4M). These results indicate that miR-196b-3p promotes CRPC development.

The expression of Meis2, a target of miR-196b-3p, is controlled by PPP3CC-directed inhibition of IκBα/p65/miR-196b

We employed DIANA-microT v5.0 program (Paraskevopoulou et al., 2013) to screen the gene candidates targeted by miR-196b-3p. Top candidates were further validated by their differential expression in PPC and CRPC cells (Figure S5A). We found that the expression of Meis2, a strong target candidate of miR-196b-3p, was significantly decreased in CRPC cells (Figure 5A and S5B). Overexpression of miR-196b in PPC cells resulted in significant decrease of Meis2 mRNA and protein expression (Figure 5B and S5C), while inhibition of miR-196b-3p in CRPC cells increased Meis2 mRNA and protein expression (Figure 5C and S5D). Furthermore, the expression of Meis2 was significantly decreased in allograft tumor tissues derived from miR-196b-overexpression Myc-CaP cells (Figure 5D and S5E). These results suggest that miR-196b-3p suppresses Meis2 expression.

Furthermore, we found that Meis2 was also regulated by PPP3CC and p65. Knockdown of PPP3CC or overexpression of p65 in PPC cells decreased the expression of Meis2 (Figure S5F), while overexpression of PPP3CC or knockdown of p65 in CRPC cells increased the expression of Meis2 (Figure S5G). MiR-196b-3p inhibitors could block PPP3CC-knockdown or p65 overexpression-mediated reduction of Meis2 expression in PPC cells (Figure 5E), while miR-196b overexpression could block PPP3CC overexpression or p65 knockdown-induced Meis2 expression in CRPC cells (Figure 5F). These results suggest that the expression of Meis2 is controlled by PPP3CC-directed inhibition of IκBα/p65/miR-196b-3p (Figure S5H).

Meis2, a member of Meis family, is a homeodomain transcription factor. A gene array study showed that the expression of Meis2 was reversely correlated with the prognosis of prostate cancer patients (Chen et al., 2012). We found that knockdown of Meis2 in PPC cells significantly increased while overexpression of Meis2 in CRPC cells significantly decreased the colony formation in soft agar and tumor sphere formation in suspension culture (Figure 5G–J and S5I–O). Meis2 stable overexpression cells developed CRPC in FVB mice much slower than control cells (Figure 5K, S5P, and S5Q). These results suggest that Meis2 suppresses CRPC development.

Meis2, PPP3CC, p65, and miR-196b form a feed-forward circuit in CRPC

Interestingly, we found Meis2 also regulate PPP3CC in CRPC cells. Knockdown of Meis2 in PPC cells by siRNA decreased PPP3CC mRNA (Figure S6A) and protein expression (Figure 6A). ChIP assay showed that the binding of Meis2 to the endogenous PPP3CC (−500/−341) promoter was decreased in CRPC cells as compared with PPC cells (Figure 6B, S6B, and Table S1), suggesting that Meis2 regulates the transcription of PPP3CC.

Given the findings that PPP3CC directs the inhibition of IκBα/p65/miR-196b, we predicted that Meis2 may also regulate p65 activity and miR-196b expression. As expected, knockdown of Meis2 in PPC cells increased p65 activity and miR-196b expression (Figure S6C and S6D), while overexpression of Meis2 in CRPC cells decreased p65 activity and miR-196b expression (Figure S6E and S6F). Furthermore, We found that the regulation of Meis2 on p65 and miR-196b was mediated by PPP3CC. Knockdown of Meis2 in PPC cells

decreased the expression of PPP3CC and induced the expression of miR-196b-3p and p65 activity, restoring the expression of PPP3CC blocked the induction of p65 activity and miR-196b-3p expression (Figure 6C and 6D). Similarly, overexpression of Meis2 in CRPC cells induced the expression of PPP3CC and reduced the expression of miR-196b-3p and p65 activity, knockdown of PPP3CC blocked the reduction of p65 activity and miR-196b-3p expression (Figure 6E and 6F). These results suggest that Meis2 controls PPP3CC-directed inhibition of IκBα/p65/miR-196b-3p. Therefore, Meis2, PPP3CC, IκBα/p65, and miR-196b form a feed-forward signaling circuit, and the constitutive activation of this signaling circuit in CRPC is not dependent on traditional NF-κB activation pathways (Figure 6G).

The constitutive signaling circuit drives the expression of cancer stem cell transcription factors in CRPC

We showed that CRPC cells were more cancer stem cell-like than PPC cells (Figure 1E–G). To examine which stem cell transcription factors are related to this phenotype, the expression of a group of stem cell transcription factors was analyzed by qRT-PCR in PPC and CRPC cells. We found that the expression of Fosl1, Gli3, Wwtr1, Twist2, Sox2, Oct4, and Nanog were increased in CRPC cells as compared with PPC cells (Figure S6G). Furthermore, knockdown of p65 or inhibition of miR-196b-3p in CRPC cells decreased (Figure 6H, 6I, and S6H) while the overexpression of p65 or miR-196b in PPC cells increased the expression of Twist2, Sox2, Oct4, and Nanog (Figure S6I and S6J). Whereas, knockdown of PPP3CC or Meis2 in PPC cells increased (Figure S6K and S6L) while overexpression of PPP3CC or Meis2 in CRPC cells decreased the expression of Twist2, Sox2, Oct4, and Nanog (Figure 6J and 6K). Consistently, the expression of Twist2, Sox2, Oct4, and Nanog protein was highly increased in CRPC cells (Figure S6M). The expression of Twist2, Sox2, Oct4, and Nanog was decreased in allograft tumors derived from p65 knockdown (Figure 6L), PPP3CC overexpression (Figure 6M), or Meis2 overexpression (Figure 6N) Myc-CaP cells while increased in allograft tumors derived from miR-196b overexpression (Figure 6O) Myc-CaP cells. These results suggest that the constitutive signaling circuit drives the expression of stem cell transcription factors, Twist2, Sox2, Oct4, and Nanog in CRPC cells.

Since p65 and Meis2 are two transcriptional factors in this constitutive signaling circuit, we asked whether p65 and/or Meis2 directly regulate the expression of stem cell transcription factors, Twist2, Sox2, Oct4, and Nanog in CRPC cells. ChIP assays showed that the binding of p65 to Twist2 promoter at −47 ~ +79 region (Figure S6N), to Sox2 promoter at +735 ~ +905 region (Figure S6O), to Oct4 promoter at +282 ~ +386 region (Figure S6P), and to Nanog promoter at −531 ~ −381 region (Figure S6Q) in CRPC cells was significantly increased as compared with PPC cells. However, no binding of Meis2 to the promoters of these stem cell transcription factors was found (Figure S6R–U). These results suggest that constitutive p65 in CRPC cells directly regulates the expression of stem cell transcription factors, Twist2, Sox2, Oct4, and Nanog in CRPC cells.

To analyze if the constitutive p65 regulates the classical NF-κB target genes in CRPC cells, we examined a group of known cancer relevant NF-κB targets, including cytokines, chemokines, cell adhesion molecules, and apoptosis related regulators (Pahl, 1999) by qRT-

PCR. We found that the expression of some of these genes was increased in CRPC cells as compared with PPC cells (Figure S6V). Knockdown of p65 in CRPC cells decreased the expression of CD44, Icam1, Ltb, Traf2, Vcam1, and Xiap (Figure S6W). The expression of some NF-κB target genes, for instance Cxcl15, were highly increased in CRPC cells, but were not decreased in p65 knocked-down CRPC cells, suggesting these genes are not regulated by constitutive NF-κB in CRPC cells.

The constitutive signaling circuit is recaptured in human prostate cancer xenograft mouse models

To exclude the possibility that the constitutive signaling circuit formed in CRPC cells is mouse model-specific, we established a human PCa xenograft mouse model. In this model an androgen-sensitive human PCa cell line, LNCaP, was inoculated into *Rag1*$^{-/-}$ mice to generate androgen-dependent primary tumors (LN-PPC), when the tumor size reached around 500 mm^3 mice were castrated, the tumor shrank and regrew. When the tumor size reached around 500 mm^3 mice were euthanized and castration-resistant tumors (LN-CRPC) were collected (Ammirante et al., 2010). We analyzed the p65 activity and the expression of p-IκBα, IκBα, PPP3CC, Meis2, and miR-196b-3p in LN-PPC and LN-CRPC cells. We found that the expression of miR-196b-3p and p-IκBα protein and the p65 activity were increased while the expression of IκBα, PPP3CC, and Meis2 protein was decreased in LN-CRPC cells as compared with LN-PPC cells (Figure 7A–C, and S7A). We also found that the expression of the stem cell transcription factors, Twist2, Sox2, Oct4, and Nanog, in LN-CRPC cells was significantly increased as compared with LN-PPC cells (Figure 7D). These results indicate that the constitutively activated feed-forward signaling circuit identified in Myc-CaP allograft mouse models also exists in human PCa LNCaP xenograft model.

The constitutive signaling circuit is manifest in human prostate tumors

To test whether the constitutive signaling circuit identified in mouse models is relevant to clinical human prostate cancer, the expression of p-IκBα protein was detected by Western blot and the expression of primary miR-196b, PPP3CC, and Meis2 mRNA was examined by qRT-PCR in 80 cases of human prostate cancer tissues. We found that the expression of p-IκBα protein in human prostate cancer tissues was positively correlated with the expression of miR-196b (Figure 7E), while reversely related to the expression of PPP3CC (Figure 7F) and Meis2 (Figure 7G). Consistently, the expression of miR-196b in human prostate cancer tissues was reversely correlated with the expression of PPP3CC (Figure 7H) and Meis2 (Figure 7I), and the expression of PPP3CC was positively correlated with the expression of Meis2 (Figure 7J). Similarly, immunohistochemistry (IHC) analysis of paraffin-embedded human prostate tumor tissue sections showed that prostate cancers with high expression of p-IκBα and nuclear p65 had low expression of PPP3CC, Meis2, and IκBα, while prostate cancers with low expression of p-IκBα and nuclear p65 had high expression of PPP3CC, Meis2, and IκBα (Figure S7B). These results suggest that the constitutive signaling circuit is manifested in human prostate cancer.

Importantly, survival time was much longer in patients having tumors with low levels of p-IκBα and miR-196b and high levels of PPP3CC and Meis2 expression (pIκBα^{Low}miR-196b^{Low}PPP3CC^{High}Meis2^{High}) than patients having tumors with high

levels of p-IκBα and miR-196b and low levels of PPP3CC and Meis2 expression (pIκBα^{High}miR-196b^{High}PPP3CC^{Low}Meis2^{Low}) (Figure 7K, 7L, and S7C). Furthermore, the expression of Twist2 (Figure S7D), Sox2 (Figure S7E), Oct4 (Figure S7F), and Nanog (Figure S7G) was significantly higher in tumors with p-IκBα^{High}miR-196b^{High}PPP3CC^{Low}Meis2^{Low} than tumors with p-IκBα^{Low}miR-196b^{Low}PPP3CC^{High}Meis2^{High}. These results support that the constitutive signaling circuit drives tumorigenicity and advanced prostate cancer development.

DISCUSSION

Several cellular and molecular mechanisms are reported related to CRPC development, including an increase in intratumoral androgen biosynthesis, aberrant AR activation, crosstalk with other oncogenic pathways, reactivation of EMT processes, and upregulation of genes that regulate stemness and self-renewal (Dutt and Gao, 2009; Karantanos et al., 2013). In the present study, we show that a constitutively activated inflammatory signaling circuit composed of IκBα/NF-κB(p65), miR-196b-3p, Meis2, PPP3CC is emerged in PCa cells during the progression from androgen-sensitive PCa to CRPC. This constitutive signaling circuit drives the high tumorigenicity of CRPC, and is correlated with the poor prognosis of prostate cancer patients.

Considerable evidences indicate that IKK/NF-κB signaling pathways are involved in carcinogenesis, cancer progression, metastasis, and drug resistance, and therefore NF-κB has been regarded as one of the most important targets for cancer therapy (Karin, 2006; Luo et al., 2005; Perkins, 2012). However, the application of IKK/NF-κB inhibitors for the treatment of human cancer is impeded by severe side effects due to the indiscriminate inhibition of IKK/NF-κB in normal immune cells. Although certain onco-viral proteins, cancer-associated chromosomal translocations, mutations, autocrine and paracrine production of proinflammatory cytokines or chronic infections can activate NF-κB in tumor cells, the mechanisms that cause and maintain the constitutive NF-κB activation in tumor cells are largely unclear, and the difference between constitutive NF-κB signaling in tumor cells and the NF-κB immune (response) signaling in normal immune cells is unknown (Rokavec and Luo, 2012; Rokavec et al., 2012). Our studies demonstrate that constitutive NF-κB activation in CRPC cells is emerged and maintained by a feed-forward signaling circuit, where the constitutive IκBα/NF-κB(p65) drives the expression of miR-196b-3p that inhibits the expression of Meis2 and PPP3CC, down-regulated PPP3CC is unable to suppress p-IκBα, leading to constitutive IκBα phosphorylation and NF-κB activation. Notably, the constitutive activation of NF-κB in CRPC cells is not dependent on traditional IKK/NF-κB activation pathways, and it is the constitutively activated NF-κB signaling circuit in PCa cells that drives CRPC development. Therefore, selective inhibition of the constitutive NF-κB in tumor cells by targeting the individual non-IκBα/NF-κB components of the constitutive signaling circuit will keep the strong anti-cancer efficacy of NF-κB inhibition while avoid NF-κB suppression in normal (immune) cells that would be highly efficient and relatively low or free of toxic side effects related to indiscriminate IKK/NF-κB inhibition.

MiR-196b is a member of the miR-196 sub-family, which comprises miR-196a and miR-196b (Chen et al., 2011). Accumulating studies demonstrates that miR-196 plays critical roles in normal development and in the pathogenesis of human diseases such as cancer (He et al., 2011; Lu et al., 2014). Our studies demonstrate that miR-196b-3p is one of the key components of the constitutively activated signaling circuit, where the expression of miR-196b-3p is driven by constitutively activated NF-κB (p65) in CRPC cells. Inhibition of miR-196b-3p suppresses while overexpression of miR-196b-3p promotes CRPC development *in vitro* and in mouse models. Several genes have been reported as the direct targets of miR-196b, including HOX-A in acute lymphoblastic leukemia (Schotte et al., 2010), HOX-C8 in breast cancer (Li et al., 2010), and NME4 (Nucleoside Diphosphate Kinase 4) in oral cancer (Lu et al., 2014). Our studies demonstrate that Meis2 is the major target of miR-196b-3p in CRPC, NF-κB-directed expression of miR-196b-3p downregulates Meis2 in CRPC cells.

Meis2 is an essential developmental gene in mammals (Kondo et al., 2014). Meis2 has been reported highly expressed in human neuroblastoma cell lines and is required for neuroblastoma cell survival and proliferation (Zha et al., 2014), whereas strong nuclear Meis2 expression is related with a better overall survival of ovarian cancer patients (Crijns et al., 2007). In human prostate cancer, Meis2 is decreased in poor-prognosis tumors (Chen et al., 2012). Our studies demonstrate that Meis2 is one of the important components of the constitutively activated signaling circuit, where it mediates NF-κB/miR-196b-3p-induced suppression of PPP3CC in CRPC cells. Overexpression of Meis2 disrupts the constitutive signaling circuit and significantly inhibits CRPC development.

It has been reported that calcineurin (also called protein phosphatase 2B or PP2B) can either increase or inhibit NF-κB activity at specific conditions in different cell-types (Pons and Torres-Aleman, 2000; Trushin et al., 1999). Our studies show that the down-regulation of PPP3CC, the calcineurin catalytic subunit γ-isoform, is related to the constitutive IκBα phosphorylation and NFκB activation in CRPC cells, PPP3CC can directly dephosphorylate p-IκBα *in vitro*. The role of PPP3CC in cancer is unclear. Prostate cancer tissue microarray data show that decreased expression of PPP3CC in prostate tumors is associated with prostate cancer recurrence (Hornstein et al., 2008). Our studies demonstrated that PPP3CC is one of the important components of the constitutive signaling circuit, where IκBα/NF-κB(p65)/miR-196b-3p/Meis2-mediated suppression of PPP3CC leads to constitutive IκBα phosphorylation and NF-κB(p65) activation in CRPC cells. Overexpression of PPP3CC disrupts the constitutive signaling circuit and significantly inhibits CRPC development.

Although it is still in debate regarding the role of cancer stem cells in primary tumorigenesis, it has been believed that one or a few cancer stem cells can generate a secondary tumor (Beck and Blanpain, 2013; Kreso and Dick, 2014). In our studies we found that the differences of tumorigenicity between PPC and CRPC cells were much bigger in allograft mouse models when mice inoculated with low cell numbers. Although there are big differences of cancer stem-like cell populations between PPC and CRPC cells, when inoculated more than 100 cells, the numbers of cancer stem cells in PPC cells is enough to generate a secondary tumor in a similar speed to CRPC cells, while when inoculated low cell

numbers (10 or 5 cells), the amount of cancer stem cells in these number of PPC cells is not enough to generate a secondary tumor in a similar speed to CRPC cells.

This highly tumorigenic feature of CRPC cells is mediated and maintained by the constitutive inflammatory feed-forward signaling circuit that controls the expression of a group of stem cell transcription factors, including Twist2, Sox2, Oct4, and Nanog. Disrupting this circuit by targeting any of its individual components blocks the expression of these transcription factors and significantly impairs CRPC development, suggesting that by riding on this constitutive signaling circuit the "power" of each individual component of this circuit is significantly amplified. Therefore, disrupting this circuit by targeting any of its individual components would be a powerful way for the suppression of CRPC.

EXPERIMENTAL PROCEDURES

Cells and reagents

Myc-CaP, an androgen sensitive prostate cancer cell line derived from *c-Myc* transgenic mouse, and LNCaP, a human prostate carcinoma cell line, were cultured in RPMI 1640 medium supplemented with 1% antibiotic-antimycotic and 10% fetal bovine serum (FBS), and incubated at 37°C in a humidified atmosp here containing 5% CO_2. The inhibitors used in the experiments were purchased from Calbiochem or Enzo Life Science. Details on cells and reagents can be found in the Supplemental Experimental Procedures.

Preparation of primary cancer cells from prostate cancer mouse models

FVB and *Rag1*$^{-/-}$ mice were obtained from The Jackson Laboratory and maintained under specific pathogen-free conditions with phytoestrogen-free food and water *ad libitum*. The mouse experimental protocols were approved by the Scripps Florida IACUC, and were followed the guidelines of the National Institute of Health. Details on preparation of primary cancer cells can be found in the Supplemental Experimental Procedures.

Prostate cancer development in animal models

FVB male mice (6 week-old) were used for allograft model. To determine the tumorigenicity of Myc-CaP, PPC, and CRPC cells, cells with series of dilution were mixed with GFR Matrigel and inoculated into FVB mice subcutaneously. Details on prostate cancer development in animal models can be found in the Supplemental Experimental Procedures.

Statistical Analysis

Differences between groups were examined for statistical significance using Student's *t* test. All *p* values are two-tailed, $p < 0.05$ was considered statistically significant.

Please refer to the Supplemental Experimental Prcoedures for more details.

Supplementary Material

Refer to Web version on PubMed Central for supplementary material.

Acknowledgments

We thank Dr. Maria Berenice Duran for critically read the manuscript. This work was supported by grants from National Institute of Health (1R01CA140956, 1R01CA197944, 1R21NS073098), the United States Department of Defense (W81XWH-09-1-0533, W81XWH-14-1-0051, W81XWH-15-1-0235), The Florida Department of Health, Bankhead-Coley Cancer Research Program (09BB-13), and the ThinkPinkKids Foundation to J.L.L., by a postdoctoral trainee fellowship from the Frenchman's Creek Women For Cancer Research to J.H.J.

References

Alibhai SM, Gogov S, Allibhai Z. Long-term side effects of androgen deprivation therapy in men with non-metastatic prostate cancer: A systematic literature review. Crit Rev Oncol Hematol. 2006

Amaral TM, Macedo D, Fernandes I, Costa L. Castration-resistant prostate cancer: mechanisms, targets, and treatment. Prostate Cancer. 2012; 2012:327253. [PubMed: 22530130]

Ammirante M, Kuraishy AI, Shalapour S, Strasner A, Ramirez-Sanchez C, Zhang W, Shabaik A, Karin M. An IKKalpha-E2F1-BMI1 cascade activated by infiltrating B cells controls prostate regeneration and tumor recurrence. Genes & development. 2013; 27:1435–1440. [PubMed: 23796898]

Ammirante M, Luo JL, Grivennikov S, Nedospasov S, Karin M. B-cell-derived lymphotoxin promotes castration-resistant prostate cancer. Nature. 2010; 464:302–305. [PubMed: 20220849]

Beck B, Blanpain C. Unravelling cancer stem cell potential. Nat Rev Cancer. 2013; 13:727–738. [PubMed: 24060864]

Chen C, Zhang Y, Zhang L, Weakley SM, Yao Q. MicroRNA-196: critical roles and clinical applications in development and cancer. J Cell Mol Med. 2011; 15:14–23. [PubMed: 21091634]

Chen JL, Li J, Kiriluk KJ, Rosen AM, Paner GP, Antic T, Lussier YA, Vander Griend DJ. Deregulation of a Hox protein regulatory network spanning prostate cancer initiation and progression. Clinical cancer research: an official journal of the American Association for Cancer Research. 2012; 18:4291–4302. [PubMed: 22723371]

Coussens LM, Werb Z. Inflammation and cancer. Nature. 2002; 420:860–867. [PubMed: 12490959]

Crijns AP, de Graeff P, Geerts D, Ten Hoor KA, Hollema H, van der Sluis T, Hofstra RM, de Bock GH, de Jong S, van der Zee AG, et al. MEIS and PBX homeobox proteins in ovarian cancer. Eur J Cancer. 2007; 43:2495–2505. [PubMed: 17949970]

Delhase M, Karin M. The I kappa B kinase: a master regulator of NF-kappa B, innate immunity, and epidermal differentiation. Cold Spring Harb Symp Quant Biol. 1999; 64:491–503. [PubMed: 11232326]

Dutt SS, Gao AC. Molecular mechanisms of castration-resistant prostate cancer progression. Future Oncol. 2009; 5:1403–1413. [PubMed: 19903068]

Ghosh S, Karin M. Missing pieces in the NF-kappaB puzzle. Cell. 2002; 109(Suppl):S81–96. [PubMed: 11983155]

Grivennikov SI, Greten FR, Karin M. Immunity, inflammation, and cancer. Cell. 2010; 140:883–899. [PubMed: 20303878]

He X, Yan YL, Eberhart JK, Herpin A, Wagner TU, Schartl M, Postlethwait JH. miR-196 regulates axial patterning and pectoral appendage initiation. Dev Biol. 2011; 357:463–477. [PubMed: 21787766]

Hornstein M, Hoffmann MJ, Alexa A, Yamanaka M, Muller M, Jung V, Rahnenfuhrer J, Schulz WA. Protein phosphatase and TRAIL receptor genes as new candidate tumor genes on chromosome 8p in prostate cancer. Cancer Genomics Proteomics. 2008; 5:123–136. [PubMed: 18460741]

Iliopoulos D, Hirsch HA, Struhl K. An epigenetic switch involving NF-kappaB, Lin28, Let-7 MicroRNA, and IL6 links inflammation to cell transformation. Cell. 2009; 139:693–706. [PubMed: 19878981]

Karantanos T, Corn PG, Thompson TC. Prostate cancer progression after androgen deprivation therapy: mechanisms of castrate resistance and novel therapeutic approaches. Oncogene. 2013; 32:5501–5511. [PubMed: 23752182]

Karin M. Nuclear factor-kappaB in cancer development and progression. Nature. 2006; 441:431–436. [PubMed: 16724054]

Kondo T, Isono K, Kondo K, Endo TA, Itohara S, Vidal M, Koseki H. Polycomb potentiates meis2 activation in midbrain by mediating interaction of the promoter with a tissue-specific enhancer. Dev Cell. 2014; 28:94–101. [PubMed: 24374176]

Kreso A, Dick JE. Evolution of the cancer stem cell model. Cell Stem Cell. 2014; 14:275–291. [PubMed: 24607403]

Li Y, Zhang M, Chen H, Dong Z, Ganapathy V, Thangaraju M, Huang S. Ratio of miR-196s to HOXC8 messenger RNA correlates with breast cancer cell migration and metastasis. Cancer Res. 2010; 70:7894–7904. [PubMed: 20736365]

Lu YC, Chang JT, Liao CT, Kang CJ, Huang SF, Chen IH, Huang CC, Huang YC, Chen WH, Tsai CY, et al. OncomiR-196 promotes an invasive phenotype in oral cancer through the NME4-JNK-TIMP1-MMP signaling pathway. Mol Cancer. 2014; 13:218. [PubMed: 25233933]

Luo JL, Kamata H, Karin M. IKK/NF-kappaB signaling: balancing life and death--a new approach to cancer therapy. J Clin Invest. 2005; 115:2625–2632. [PubMed: 16200195]

Luo JL, Tan W, Ricono JM, Korchynskyi O, Zhang M, Gonias SL, Cheresh DA, Karin M. Nuclear cytokine-activated IKKalpha controls prostate cancer metastasis by repressing Maspin. Nature. 2007; 446:690–694. [PubMed: 17377533]

Mulero MC, Ferres-Marco D, Islam A, Margalef P, Pecoraro M, Toll A, Drechsel N, Charneco C, Davis S, Bellora N, et al. Chromatin-bound IkappaBalpha regulates a subset of polycomb target genes in differentiation and cancer. Cancer cell. 2013; 24:151–166. [PubMed: 23850221]

Mulholland DJ, Xin L, Morim A, Lawson D, Witte O, Wu H. Lin-Sca-1+CD49fhigh stem/progenitors are tumor-initiating cells in the Pten-null prostate cancer model. Cancer Res. 2009; 69:8555–8562. [PubMed: 19887604]

Pahl HL. Activators and target genes of Rel/NF-kappaB transcription factors. Oncogene. 1999; 18:6853–6866. [PubMed: 10602461]

Paraskevopoulou MD, Georgakilas G, Kostoulas N, Vlachos IS, Vergoulis T, Reczko M, Filippidis C, Dalamagas T, Hatzigeorgiou AG. DIANA-microT web server v5.0: service integration into miRNA functional analysis workflows. Nucleic acids research. 2013; 41:W169–173. [PubMed: 23680784]

Perkins ND. The diverse and complex roles of NF-kappaB subunits in cancer. Nat Rev Cancer. 2012; 12:121–132. [PubMed: 22257950]

Pons S, Torres-Aleman I. Insulin-like growth factor-I stimulates dephosphorylation of ikappa B through the serine phosphatase calcineurin (protein phosphatase 2B). The Journal of biological chemistry. 2000; 275:38620–38625. [PubMed: 10973957]

Rokavec M, Luo JL. The transient and constitutive inflammatory signaling in tumorigenesis. Cell Cycle. 2012; 11:2587–2588. [PubMed: 22751429]

Rokavec M, Wu W, Luo JL. IL6-mediated suppression of miR-200c directs constitutive activation of inflammatory signaling circuit driving transformation and tumorigenesis. Molecular cell. 2012; 45:777–789. [PubMed: 22364742]

Schotte D, Lange-Turenhout EA, Stumpel DJ, Stam RW, Buijs-Gladdines JG, Meijerink JP, Pieters R, Den Boer ML. Expression of miR-196b is not exclusively MLL-driven but is especially linked to activation of HOXA genes in pediatric acute lymphoblastic leukemia. Haematologica. 2010; 95:1675–1682. [PubMed: 20494936]

Shi Y. Serine/threonine phosphatases: mechanism through structure. Cell. 2009; 139:468–484. [PubMed: 19879837]

Trushin SA, Pennington KN, Algeciras-Schimnich A, Paya CV. Protein kinase C and calcineurin synergize to activate IkappaB kinase and NF-kappaB in T lymphocytes. The Journal of biological chemistry. 1999; 274:22923–22931. [PubMed: 10438457]

Watson PA, Ellwood-Yen K, King JC, Wongvipat J, Lebeau MM, Sawyers CL. Context-dependent hormone-refractory progression revealed through characterization of a novel murine prostate cancer cell line. Cancer Res. 2005; 65:11565–11571. [PubMed: 16357166]

Xin L, Lawson DA, Witte ON. The Sca-1 cell surface marker enriches for a prostate-regenerating cell subpopulation that can initiate prostate tumorigenesis. Proc Natl Acad Sci U S A. 2005; 102:6942–6947. [PubMed: 15860580]

Zha Y, Xia Y, Ding J, Choi JH, Yang L, Dong Z, Yan C, Huang S, Ding HF. MEIS2 is essential for neuroblastoma cell survival and proliferation by transcriptional control of M-phase progression. Cell Death Dis. 2014; 5:e1417. [PubMed: 25210800]

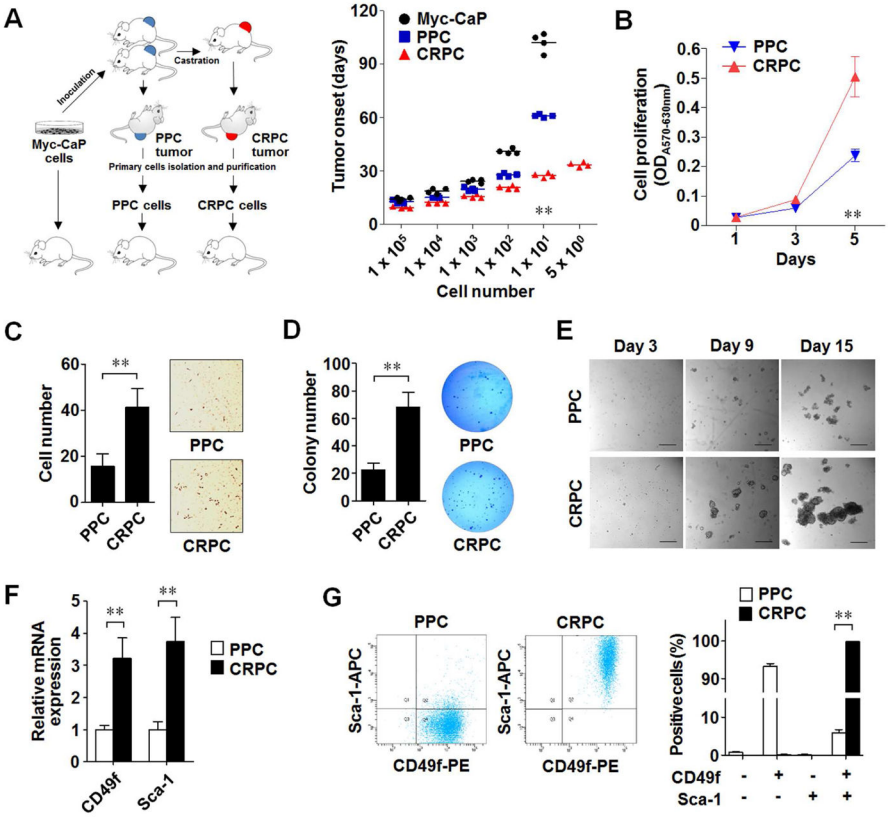

Figure 1. CRPC cells are highly tumorigenic and cancer stem cell-like

(A) Tumorigenicity analysis in FVB male mice inoculated with indicated numbers of cultured Myc-CaP cells or primary cells purified from primary Myc-CaP allograft tumor (PPC) or castration-resistant Myc-CaP allograft tumor (CRPC).

(B) MTT assay for cell proliferation rates of PPC and CRPC cells.

(C) Transwell migration analysis of PPC and CRPC cells.

(D) Soft agar colony formation analysis of PPC and CRPC cells.

(E) Tumor sphere formation analysis of PPC and CRPC cells. Scale bars represent 100 μm.

(F) qRT-PCR analysis of *CD49f* and *Sca-1* mRNA expression in PPC and CRPC cells

(G) Fluorescence-activated cell sorter (FACS) analysis of CD49f and Sca-1 positive populations of PPC and CRPC cells.

The results in (B)–(D), (F), and (G) represent the mean ± SD of three independent experiments performed in triplicate. Statistically significant differences are indicated. (**) $p < 0.01$. See also Figure S1.

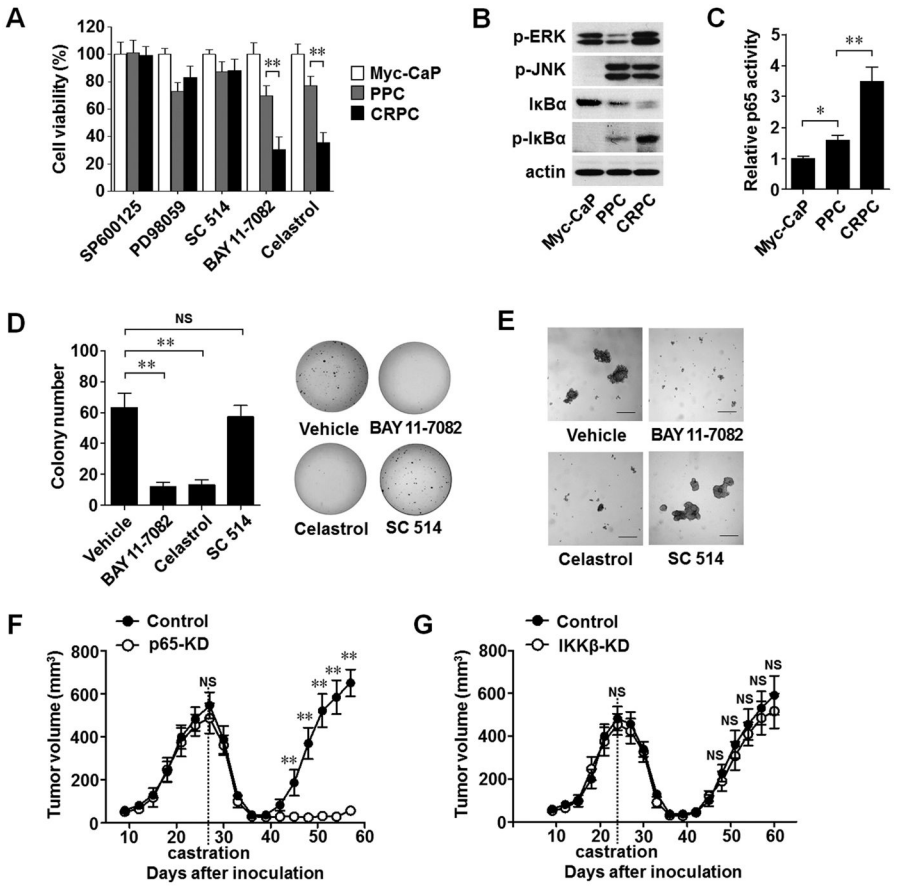

Figure 2. IKKβ-independent constitutive NF-κB/p65 activation drives CRPC development

(A) MTT cell viability analysis of Myc-CaP, PPC, and CRPC cells treated with indicated inhibitors for 72 hr.

(B) Western blot analysis of indicated protein in Myc-CaP, PPC, and CRPC cells.

(C) ELISA analysis of NF-κB (p65) activity in Myc-CaP, PPC, and CRPC cells.

(D) Soft agar colony formation analysis (Left panel) and the phase contrast images of the colonies (Right panel) of CRPC cells treated with the indicated inhibitors.

(E) Tumor sphere formation analysis of CRPC cells treated with the indicated inhibitors. Scale bars represent 100 μm.

(F) Allograft tumor development in FVB male mice inoculated with control or p65 stable knockdown (p65-KD) Myc-CaP cells ($n = 5$). When tumors reached 500 mm^3, mice were castrated. Tumor volume was measured every 3 days.

(G) Allograft tumor development in FVB male mice inoculated with control or IKKβ stable knockdown (IKKβ-KD) Myc-CaP cells ($n = 5$). When tumors reached 500 mm^3, mice were castrated.

The results in (A), (C), and (D) represent the mean ± SD of three independent experiments performed in triplicate. Statistically significant differences are indicated. (*) $p < 0.05$; (**) $p < 0.01$. See also Figure S2.

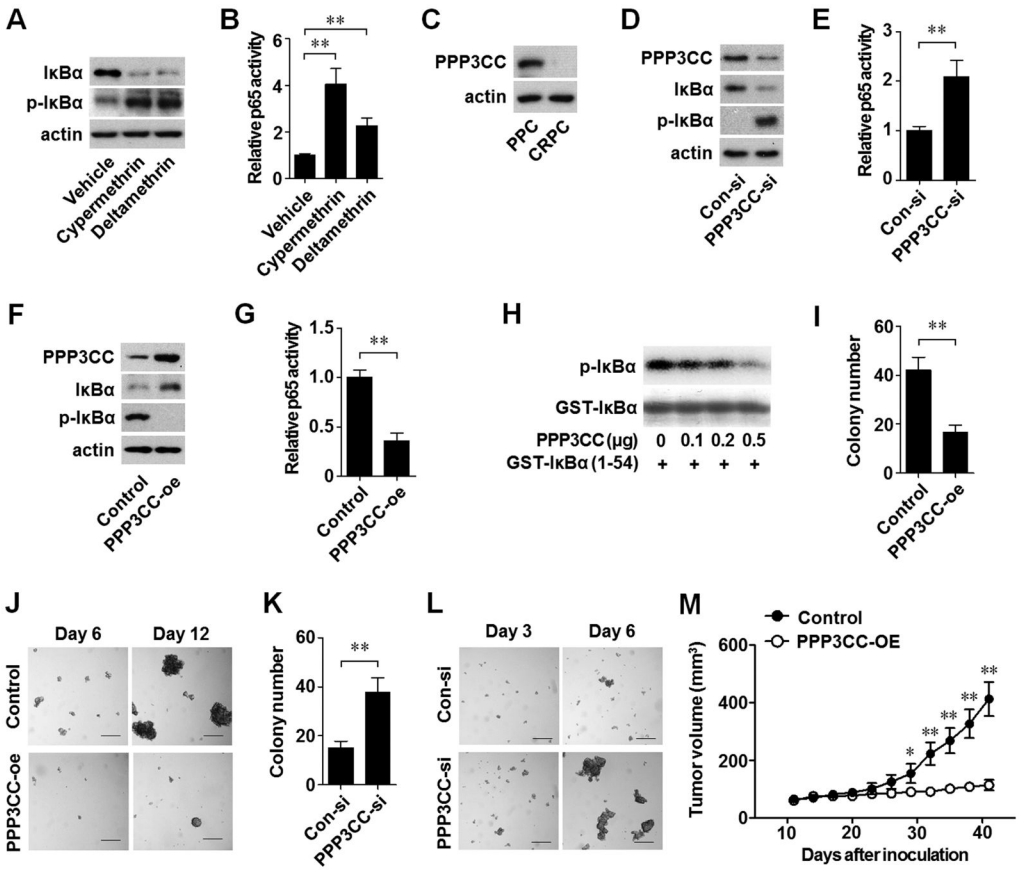

Figure 3. PPP3CC suppression leads to constitutive NF-κB/p65 activation and CRPC development

(A) Western blot analysis of IκBα and p-IκBα expression in PPC cells treated with vehicle, cypermethrin, or deltamethrin for 72 hr.

(B) ELISA analysis of NF-κB (p65) activity in PPC cells treated with vehicle, cypermethrin, or deltamethrin for 72 hr.

(C) Western blot analysis of PPP3CC expression in PPC and CRPC cells.

(D) Western blot analysis of IκBα and p-IκBα expression in PPC cells transfected with scrambled (Con-si) or PPP3CC siRNA (PPP3CC-si) for 48 hr.

(E) ELISA analysis of NF-κB (p65) activity in PPC cells transfected with indicated siRNA for 48 hr.

(F) Western blot analysis of IκBα and p-IκBα expression in CRPC cells transfected with control vector (Control) or PPP3CC expression plasmid (PPP3CC-oe) for 48 hr.

(G) ELISA analysis of NF-κB (p65) activity in CRPC cells transfected with indicated plasmid for 48 hr.

(H) *In vitro* dephosphorylation of GST-IκBα-^{32}P protein by PPP3CC protein.

(I) Soft agar colony formation analysis of CRPC cells transfected with indicated plasmid.

(J) Tumor sphere formation analysis of CRPC cells transfected with indicated plasmid. Scale bars represent 100 μm.

(K) Soft agar colony formation analysis of PPC cells transfected with indicated siRNA.

(L) Tumor sphere formation analysis of PPC cells transfected with indicated siRNA. Scale bars represent 100 μm.

(M) Allograft tumor development in castrated FVB male mice inoculated with control or PPP3CC overexpression (PPP3CC-OE) Myc-CaP cells ($n = 5$).

The results in (B), (E), (G), (I), and (K) represent the mean ± SD of three independent experiments performed in triplicate. Statistically significant differences are indicated. (*) $p < 0.05$; (**) $p < 0.01$. See also Figure S3.

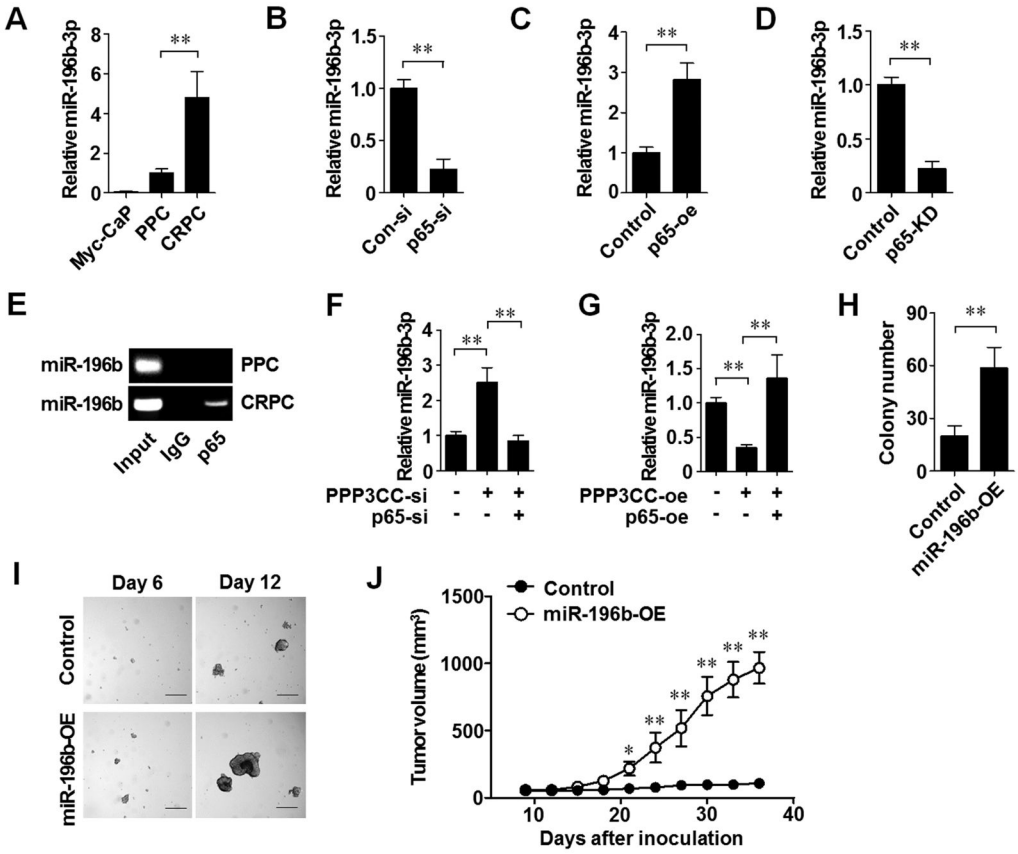

Figure 4. PPP3CC downregulation-mediated constitutive NF-κB/p65 controls miR-196b-3p expression in CRPC

(A) The expression of miR-196b-3p in Myc-CaP, PPC, and CRPC cells.

(B) The expression of miR-196b-3p in CRPC cells transfected with scrambled (Con-si) or p65 siRNA (p65-si) for 48 hr.

(C) The expression of miR-196b-3p in PPC cells transfected with control vector (Control) or p65 expression plasmid (p65-oe) for 48 hr.

(D) The expression of miR-196b-3p in castration-resistant allograft tumors derived from Myc-CaP cells without (Control) or with p65 stable knockdown (p65-KD).

(E) ChIP assay for p65 protein binding to miR-196b promoter in PPC and CRPC cells.

(F) The expression of miR-196b-3p in PPC cells transfected with scrambled (Con-si) or PPP3CC siRNA (PPP3CC-si), 24 hr later followed by transfection with p65 siRNA (p65-si) for 48 hr.

(G) The expression of miR-196b-3p in CRPC cells transfected with empty vector or PPP3CC expression plasmid (PPP3CC-oe), 24 hr later followed by transfection with p65 expression plasmid (p65-oe) for 48 hr.

(H) Soft agar colony formation analysis of control or miR-196b overexpression (miR-196b-OE) Myc-CaP cells.

(I) Tumor sphere formation analysis of control or miR-196b overexpression (miR-196b-OE) Myc-CaP cells. Scale bars represent 100 μm.

(J) Allograft tumor development in castrated FVB male mice inoculated with control or miR-196b overexpression (miR-196b-OE) Myc-CaP cells ($n = 5$). Tumor volume was measured every 3 days.

The results in (A)–(D), and (F)–(H) represent the mean ± SD of three independent experiments performed in triplicate. Statistically significant differences are indicated. (*) $p < 0.05$; (**) $p < 0.01$. See also Figure S4.

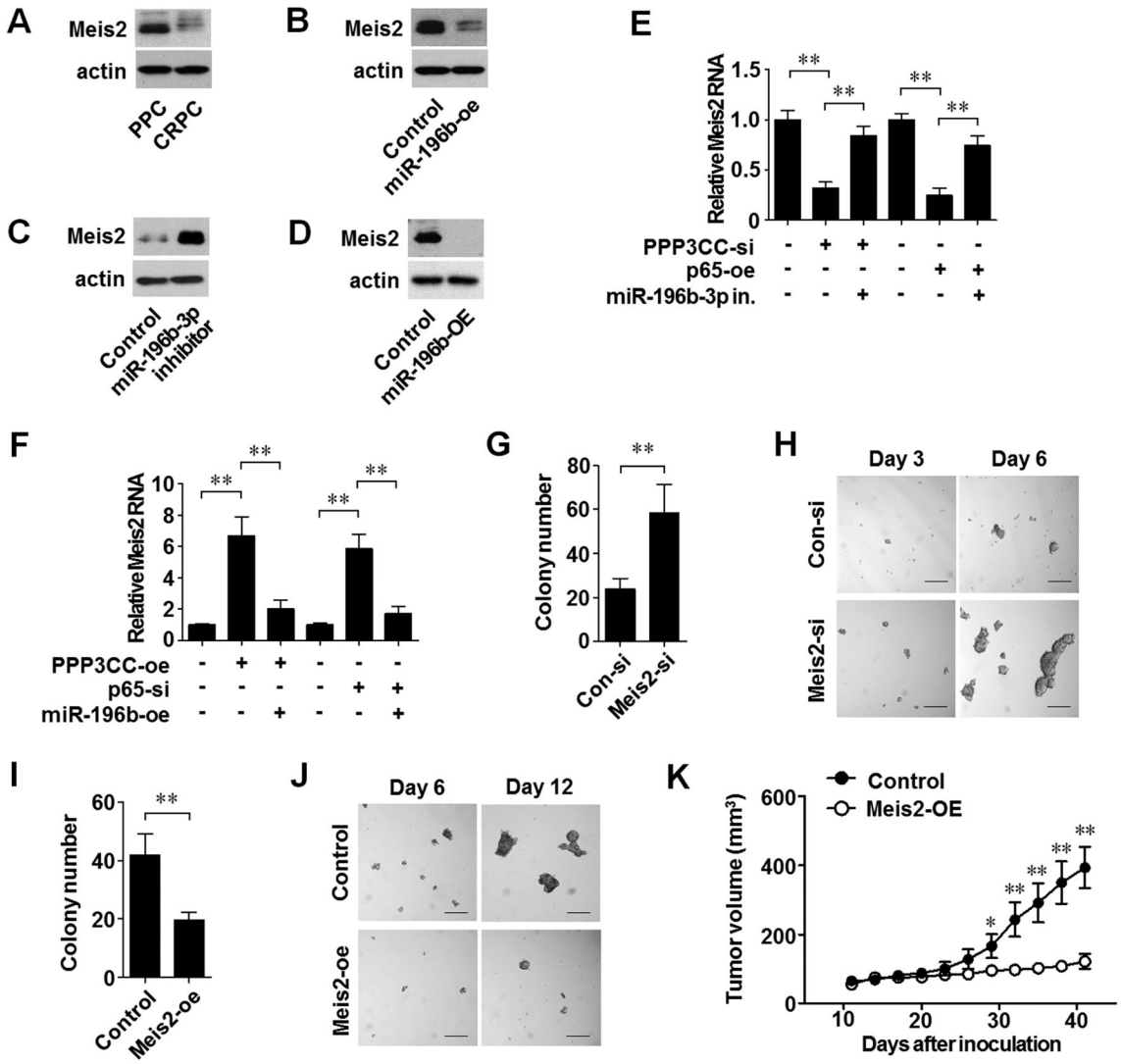

Figure 5. PPP3CC, Meis2, miR-196b, p65, and IκBα form a constitutively activated feed-forward circuit in CRPC

(A) Western blot analysis of Meis2 expression in PPC and CRPC cells.

(B) Western blot analysis of Meis2 expression in PPC cells transfected with control vector (Control) or miR-196b expression plasmid (miR-196b-oe) for 48 hr.

(C) Western blot analysis of Meis2 expression in CRPC cells treated with control or miR-196b-3p inhibitor for 48 hr.

(D) Western blot analysis of Meis2 expression in allograft tumors derived from Myc-CaP cells expressing miR-196b (miR-196b-OE) or control vector (Control).

(E) qRT-PCR analysis of *Meis2* mRNA expression in PPC cells transfected with control, Meis2 siRNA (Meis2-si), or p65 expression plasmid (p65-oe), 24 hr later followed by transfection with miR-196b-3p inhibitor for 48 hr.

(F) qRT-PCR analysis of *Meis2* mRNA expression in CRPC cells transfected with control, PPP3CC expression plasmid (PPP3CC-oe), or p65 siRNA (p65-si), 24 hr later followed by transfection with miR-196b expression plasmid (miR-196b-oe) for 48 hr.

(G) Soft agar colony formation analysis of PPC cells transfected with scrambled (Con-si) or Meis2 siRNA (Meis2-si).

(H) Tumor sphere formation analysis of PPC cells transfected with indicated siRNA. Scale bars represent 100 μm.

(I) Soft agar colony formation analysis of PPC cells transfected with control vector (Control) or Meis2 expression plasmid (Meis2-oe).

(J) Tumor sphere formation analysis of CRPC cells transfected with indicated plasmid. Scale bars represent 100 μm.

(K) Allograft tumor development in castrated FVB male mice inoculated with control or Meis2 overexpression (Meis2-OE) Myc-CaP cells ($n = 5$).

The results in (E)–(G), and (I) represent the mean ± SD of three independent experiments performed in triplicate. Statistically significant differences are indicated. (*) $p < 0.05$; (**) $p < 0.01$. See also Figure S5.

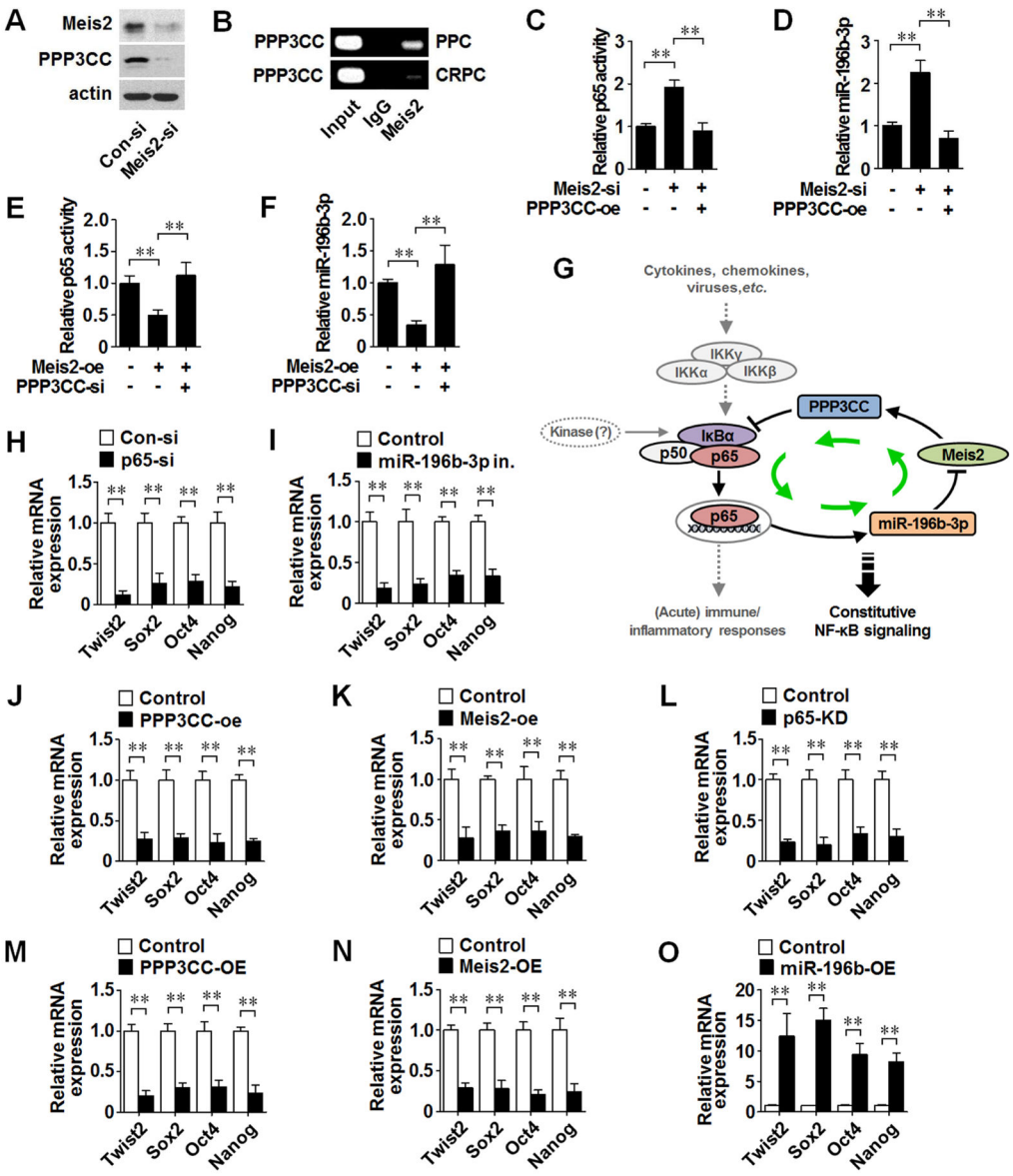

Figure 6. PPP3CC/p-IκBα/p65/miR-196b/Meis2 circuit promotes the expression of stem cell transcription factors in CRPC

(A) Western blot analysis of PPP3CC expression in PPC cells transfected with scrambled (Con-si) or Meis2 siRNA (Meis2-si) for 48 hr.

(B) ChIP assay for Meis2 protein binding to PPP3CC promoter in PPC and CRPC cells.

(C) ELISA analysis of NF-κB (p65) activity in PPC cells transfected with scrambled or Meis2 siRNA (Meis2-si), 24 hr later followed by transfection with PPP3CC expression plasmid (PPP3CC-oe) for 48 hr.

(D) The expression of miR-196b-3p in PPC cells transfected with scrambled or Meis2 siRNA (Meis2-si), 24 hr later followed by transfection with PPP3CC expression plasmid (PPP3CC-oe) for 48 hr.

(E) ELISA analysis of NF-κB (p65) activity in CRPC cells transfected with control vector or Meis2 expression plasmid (Meis2-oe), 24 hr later followed by transfection with PPP3CC siRNA (PPP3CC-si) for 48 hr.

(F) The expression of miR-196b-3p in CRPC cells transfected with control vector or Meis2 expression plasmid (Meis2-oe), 24 hr later followed by transfection with PPP3CC siRNA (PPP3CC-si) for 48 hr.

(G) Diagram of constitutively activated feed-forward signaling circuit in CRPC.

(H, I) qRT-PCR analysis of *Twist*, *Sox2, Oct4, and Nanog* mRNA expression in CRPC cells transfected with scrambled (Con-si) or p65 siRNA (p65-si) for 48 hr (H), or with control or miR-196b-3p inhibitor (miR-196b-3p in.) for 48 hr (I).

(J, K) qRT-PCR analysis of *Twist*, *Sox2, Oct4, and Nanog* mRNA expression in CRPC cells transfected with control vector (Control), PPP3CC expression plasmid (PPP3CC-oe) (J), or Meis2 expression plasmid (Meis2-oe) (K) for 48 hr.

(L–O) qRT-PCR analysis of *Twist*, *Sox2, Oct4, and Nanog* mRNA expression in castration-resistant allograft tumors derived from Myc-CaP cells without (Control) or with p65 stable knockdown (p65-KD) (L), or without (Control) or with PPP3CC stable overexpression (PPP3CC-OE) (M), or without (Control) or with Meis2 stable overexpression (Meis2-OE) (N), or without (Control) or with miR-196b stable overexpression (miR-196b-OE) (O).

The results in (C)–(F), and (H)–(O) represent the mean ± SD of three independent experiments performed in triplicate. Statistically significant differences are indicated. (**) $p < 0.01$. See also Figure S6.

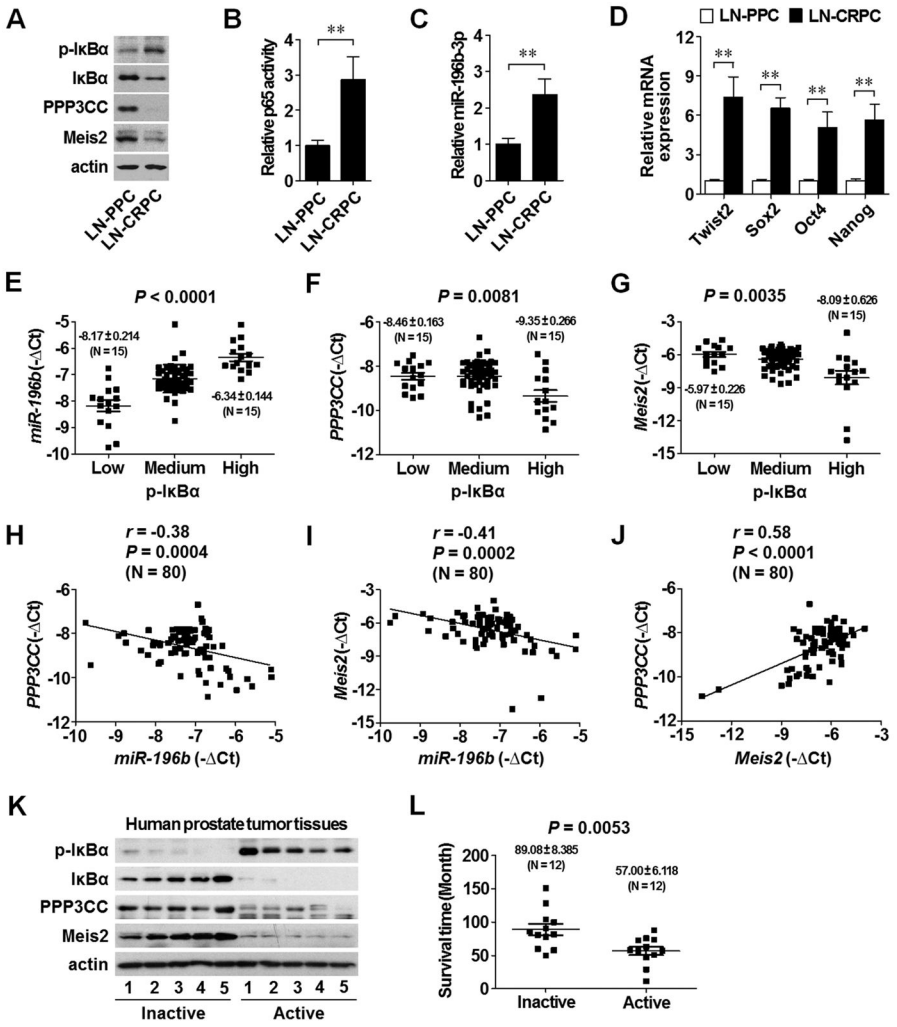

FIGURE 7. The PPP3CC/p-IκBα/p65/miR-196b/Meis2 circuit is manifested in human prostate cancers

(A) Western blot analysis of indicated proteins in primary cells purified from primary (LN-PPC) or castration-resistant (LN-CRPC) LNCaP xenograft tumors in *Rag1*$^{-/-}$ mice.

(B) ELISA analysis of NF-κB (p65) activity in LN-PPC and LN-CRPC cells.

(C) The expression of miR-196b-3p in LN-PPC and LN-CRPC cells.

(D) qRT-PCR analysis of *Twist2, Sox2, Oct4,* and *Nanog* mRNA expression in LN-PPC and LN-CRPC cells.

(E–G) Correlation analysis of p-IκBα protein expression with the expression of *miR-196b* (E), *PPP3CC* (F), or *Meis2* (G) in human prostate tumor tissues (n = 80). The expression of p-IκBα protein was analyzed by western blot, and the expression of *miR-196b*, *PPP3CC*, *Meis2* was determined by qRT-PCR. The data are presented as Mean ± SEM, and significance was calculated using the Student's t-test.

(H–J) The correlations between *miR-196b* and *PPP3CC* (H), or between *miR-196b* and *Meis2* (I), or between *Meis2* and *PPP3CC* (J) expression in human prostate cancer tissues (n = 80). The expression of *miR-196b*, *PPP3CC*, and *Meis2* was determined by qRT-PCR. Spearman correlation coefficient with the respective significance is indicated.

(K) Western blot analysis for the expression of indicated protein expression in human prostate cancer tissues.

(L) Correlation analysis of survival time in circuit-dependent (inactive, $n = 12$; active, $n = 12$) human prostate tumor tissues. The data are presented as Mean ± SEM, and significance was calculated using the Student's *t*-test.

The results in (B)–(D) represent the mean ± SD of three independent experiments performed in triplicate. Statistically significant differences are indicated. (**) $p < 0.01$. See also Figure S7.